

## LINEAR AND SECOND-ORDER EVOLUTION OF COSMIC BARYON PERTURBATIONS BELOW $10^6$ SOLAR MASSES

SHWETABH SINGH AND CHUNG-PEI MA

Department of Physics and Astronomy, University of Pennsylvania, 209 South 33rd Street, Philadelphia, PA 19104; and Department of Astronomy,  
University of California at Berkeley, 601 Campbell Hall, Berkeley, CA 94720; shwetabh@hep.upenn.edu, cpma@astron.berkeley.edu

Received 2001 September 13; accepted 2001 November 21

### ABSTRACT

Studies of the growth of cosmic perturbations are typically focused on galactic scales and above. In this paper we investigate the evolution of perturbations in baryons, photons, and dark matter for masses below  $10^6 M_\odot$  (or wavenumbers above  $100 \text{ Mpc}^{-1}$ ). Fluctuations on these scales are of interest and importance because they grow to become the earliest collapsed objects and provide the first light sources in the so-called dark ages. We investigate both the linear evolution and the second-order nonlinear effects arising from the coupling of large-scale velocity fields to small-scale perturbations in the baryon density and the electron ionization fraction. We find that this second-order nonlinear coupling dominates the growth of perturbations with masses  $\lesssim 10^3 M_\odot$  immediately after recombination, enhancing the baryon fluctuation amplitudes by a factor of  $\sim 5$ , but the nonlinear effect does not persist at late times.

*Subject headings:* cosmology: theory — early universe — large-scale structure of universe

### 1. INTRODUCTION

Theories of structure formation are aimed at describing how gravity affects the distribution of matter in the universe. The currently accepted paradigm is that gravitational instabilities amplify fluctuations imprinted in the cosmological matter and radiation density in the early universe, and these fluctuations eventually evolve into the observed web of cosmic structures. By assuming these fluctuations to be small, a linear perturbation theory can be formulated and solved. The linear theory for a perturbed Friedmann-Robertson-Walker metric was developed by Lifshitz (1946). The theory and subsequent modifications have been applied to a large number of cosmological problems and are described in detail in several textbooks (e.g., Weinberg 1972; Peebles 1980; Peacock 1999).

Most calculations and analyses based on the cosmological linear perturbation theory are focused on galactic scales or above at masses of  $M \gtrsim 10^9 M_\odot$ , or wavenumbers of  $k \lesssim 10 \text{ Mpc}^{-1}$ . This is likely due to the fact that quantities such as the mass-fluctuation power spectrum can be determined observationally only on these large scales and that the computations become expensive at high wavenumbers due to the rapid oscillations in the perturbed fields. The theory, however, is equally valid for small scales, and the evolution of  $M \lesssim 10^6 M_\odot$  perturbations is key to understanding the formation of the first-generation objects in the high-redshift universe. A detailed study of perturbation modes up to  $k \sim 1000 \text{ Mpc}^{-1}$  has found interesting features in the linear baryon field (Yamamoto, Sugiyama, & Sato 1998). For example, the tight coupling between baryons and photons, which is assumed until the epoch of recombination in most calculations, breaks down well before recombination on these very small scales. This allows the baryon density field to grow substantially by recombination under the influence of the cold dark matter (CDM). This behavior is contrary to the common notion that the baryon fluctuations are wiped out by photon diffusion or Silk damping (Silk 1968) on small scales. After recombination, on the other hand, perturbation modes with  $k \gtrsim 300 \text{ Mpc}^{-1}$  are below the Jeans mass and exhibit oscillatory behavior, in contrast

to the lower  $k$  modes, which grow via Jeans instability immediately after recombination. This retards the baryon growth until the mode becomes Jeans unstable again at a later time.

Beyond the linear order, there have been recent discussions regarding nontrivial second-order effects that can enhance the linear growth of fluctuations on very small scales during recombination (Shaviv 1998; Liu et al. 2001). This nonlinear effect arises from the coupling of the large-scale velocity fields to the perturbations in the baryon density  $\delta_b$  and the electron ionization fraction  $\delta_{x_e}$  on small scales. An amplification of  $\sim 10^4$  in  $\delta_b$  has been reported (Shaviv 1998), although a more in-depth analysis (Liu et al. 2001) has found that the dramatic increase in the baryon amplitude is a result of neglecting the electron-photon diffusion term, which when included would reduce the nonlinear enhancement to a factor of  $\sim 10$ . More specifically, Shaviv (1998) showed that the timescale governing the growth of small-scale perturbations in the baryon density is  $\sim \tau_R^2/\tau_0$ , where  $\tau_R$  is the characteristic timescale for the second-order terms that are important during and immediately after recombination and  $\tau_0$  is the timescale for acoustic oscillations in the baryon fluid. He took the timescale  $\tau_D$  for momentum transfer (or diffusion) between electrons and photons due to Thomson scattering to be much larger than  $\tau_R^2/\tau_0$ . Liu et al. (2001) pointed out that this assumption is invalid during recombination since  $\tau_D \sim \tau_R^2/\tau_0$ , and  $\tau_D$  cannot be ignored. In addition, Shaviv (1998) used the Saha equation to evaluate  $\delta_{x_e}$ , which is needed to calculate  $\tau_R$ . Liu et al. (2001) instead used a rate equation for  $\delta_{x_e}$  because the assumption of thermal equilibrium required for the validity of the Saha equation does not hold during recombination. They then assumed a waveform solution for the baryon density field  $\delta_b \propto \exp(\omega\tau - ikx)$  and estimated the growth of  $\delta_b$  from the real part of  $\omega$ , which they obtained from the dispersion relation given by the baryon fluid equation.

In this paper we investigate this small-scale nonlinear phenomenon in its full extent by using the complete cosmological perturbation theory. Our work differs from Liu et al. (2001) in that instead of tracking only the real part of  $\delta_b$  from the dispersion relation, we calculate the evolution of

the perturbations in all particle species (baryons, photons, CDM, and neutrinos) at high wavenumbers  $k > 1000 \text{ Mpc}^{-1}$  by solving the complete set of Einstein and Boltzmann equations consistently. We use the linear Boltzmann code in the COSMICS package (Ma & Bertschinger 1995; Bertschinger 1995) and incorporate the aforementioned nonlinear effects by adding second-order contributions to the photon-electron momentum-transfer terms due to Thomson scattering. For consistency, we include these terms in the evolution equations for photons as well as baryons. This approach allows us to take into account possible nonlinear coupling effects and to calculate the growth, decay, and oscillations in all particle species accurately.

In § 2.1 we summarize the key portions of the linear cosmological perturbation theory. In § 2.2 we introduce the nonlinear coupling terms in the baryon and photon equations as well as the equations for the perturbed ionization fraction. Numerical results for the linear and the nonlinear evolution of four representative high- $k$  modes,  $k = 1000, 2500, 5000,$  and  $10,000 \text{ Mpc}^{-1}$ , are presented in § 3. The corresponding masses are  $\sim 1000, 64, 8,$  and  $1 M_\odot$ , respectively. Section 4 includes a discussion of the physical origin of this phenomenon and the reason why a second-order term could dominate the growth of perturbations at the era of recombination.

## 2. COSMOLOGICAL PERTURBATION THEORY

### 2.1. Linear Perturbations

The discussion here is restricted to the scalar modes of metric perturbations. We work in the conformal Newtonian gauge

$$ds^2 = a^2(\tau) [-(1 + 2\psi)d\tau^2 + (1 - 2\phi)dx^2], \quad (1)$$

where  $\phi$  and  $\psi$  are the two scalar potentials that characterize the perturbations,  $\tau$  is the conformal time,  $x$  are the spatial dimensions, and  $a$  is the scale factor. The scalar potential  $\psi$  has a simple physical interpretation of being the gravitational potential in the Newtonian limit, and  $\phi \approx \psi$  in the absence of massive neutrinos.

We solve the full set of linear evolution equations for small perturbations in the metric and the phase-space distributions of CDM, photons, baryons, and neutrinos. The full theory in this gauge is described in detail in Mukhanov, Feldman, & Brandenberger (1992) and Ma & Bertschinger (1995); here we write out only the lowest two velocity moments of the phase-space distribution for CDM (subscript  $C$ ), baryons ( $b$ ), and photons ( $\gamma$ ), which are the key quantities in this study. In  $k$ -space, we have

$$\begin{aligned} \delta_C &= -\theta_C + 3\dot{\phi}, \\ \dot{\theta}_C &= -\frac{\dot{a}}{a}\theta_C + k^2\psi, \\ \dot{\delta}_b &= -\theta_b + 3\dot{\phi}, \\ \dot{\theta}_b &= -\frac{\dot{a}}{a}\theta_b + c_s^2 k^2 \delta_b + k^2\psi + \frac{4\bar{\rho}_\gamma}{3\bar{\rho}_b} a\bar{n}_e \sigma_T (\theta_\gamma - \theta_b), \\ \dot{\delta}_\gamma &= -\frac{4}{3}\theta_\gamma + 4\dot{\phi}, \\ \dot{\theta}_\gamma &= k^2 \left( \frac{1}{4}\delta_\gamma - \sigma_\gamma \right) + k^2\psi + a\bar{n}_e \sigma_T (\theta_b - \theta_\gamma), \end{aligned} \quad (2)$$

where  $\delta$  is the density fluctuation,  $\theta = i\mathbf{k} \cdot \mathbf{v}$  is the divergence of the fluid velocity, and  $\sigma_\gamma$  is the shear stress of the photon

field, which is coupled to higher moments not written down here. On the right-hand side,  $\sigma_T$  is the Thomson scattering cross section,  $c_s$  is the baryon sound speed,  $\bar{n}_e$  is the mean electron number density, and  $\bar{\rho}_\gamma$  and  $\bar{\rho}_b$  are the mean photon and baryon energy densities. Dots denote derivatives with respect to the conformal time, and the densities and wavenumbers are all comoving. Massive neutrinos have no direct coupling to the nonlinear terms considered here, so we do not include them.

Additional equations are needed to calculate  $\bar{n}_e$ . We define the mean ionization fraction  $\bar{x}_e$  as

$$\bar{x}_e \equiv \frac{\bar{n}_e}{\bar{n}_H} = \frac{\bar{n}_e m_p}{(1-y)\bar{\rho}_b}, \quad (3)$$

where  $\bar{n}_H$  is the mean hydrogen number density,  $y$  is the primordial helium mass fraction, and  $m_p$  is the proton mass. The value  $\bar{x}_e = 1$  corresponds to complete hydrogen ionization and neutral helium, and  $\bar{x}_e$  can exceed unity when helium is ionized at an earlier time. We choose this convention for convenience because for the redshift of interest to this paper, hydrogen is the dominant source of free electrons. For times much before recombination,  $\bar{x}_e$  obeys the equilibrium Saha equation to a good approximation:

$$\frac{\bar{x}_e^2}{1 - \bar{x}_e} = \frac{1}{\bar{n}_H} \left( \frac{m_e k_B T_b}{2\pi\hbar^2} \right)^{3/2} e^{-13.6 \text{ eV}/k_B T_b}. \quad (4)$$

Here  $T_b$  is the baryon temperature,  $k_B$  is the Boltzmann constant,  $m_e$  is the electron mass, and  $\hbar$  is Planck's constant. During recombination, the rapidly declining free-electron density leads to a breakdown of ionization equilibrium, and one must integrate the appropriate kinetic equations. We use the recombination rate equation (Peebles 1968; Spitzer 1978),

$$\frac{d\bar{x}_e}{d\tau} = aC_r [\beta(T_b)(1 - \bar{x}_e) - \bar{n}_H \alpha^{(2)}(T_b) \bar{x}_e^2], \quad (5)$$

where the collisional ionization rate from the ground state is

$$\beta(T_b) = \left( \frac{m_e k_B T_b}{2\pi\hbar^2} \right)^{3/2} e^{-13.6 \text{ eV}/k_B T_b} \alpha^{(2)}(T_b), \quad (6)$$

and the recombination rate to the excited states is

$$\begin{aligned} \alpha^{(2)} &= \frac{64\pi}{(27\pi)^{1/2}} \frac{e^4}{m_e^2 c^3} \left( \frac{k_B T_b}{13.6 \text{ eV}} \right)^{-1/2} \phi_2(T_b), \\ \phi_2(T_b) &= 0.448 \ln \left( \frac{13.6 \text{ eV}}{k_B T_b} \right). \end{aligned} \quad (7)$$

Here  $e$  is the electron charge and  $c$  is the speed of light. The net recombination rate to the ground state is reduced by the fact that an atom in the  $n = 2$  level may be ionized before it decays to the ground state. The Peebles' reduction factor  $C_r$  is the ratio of the net decay rate to the sum of the decay and ionization rates from the  $n = 2$  level,

$$C_r = \frac{\Lambda_\alpha + \Lambda_{2s \rightarrow 1s}}{\Lambda_\alpha + \Lambda_{2s \rightarrow 1s} + \beta^{(2)}(T_b)}, \quad (8)$$

where

$$\begin{aligned} \beta^{(2)}(T_b) &= \beta(T_b) e^{hc/k_B T_b \lambda_\alpha}, \quad \Lambda_\alpha = \frac{8\pi\dot{a}}{a^2 n_{1s} \lambda_\alpha^3}, \\ \lambda_\alpha &= 1.216 \times 10^{-5}, \end{aligned} \quad (9)$$

$\Lambda_{2s \rightarrow 1s}$  is the rate at which net recombination occurs through two-photon decay from the  $2s$  level and is equal to 8.227

$s^{-1}$ , and  $n_{1s}$  is the number density of hydrogen atoms in the  $1s$  state.

### 2.2. Second-Order Perturbations

A complete list of second-order nonlinear contributions in perturbation theory includes many terms, but the dominant contribution comes from the terms of the order of  $\delta_b v_b$  (e.g., Hu, Scott, & Silk 1994; Dodelson & Jubas 1995). The other second-order terms are proportional to  $v_b^2$ , which are suppressed because  $v_b \sim \delta_b/k\tau \ll \delta_b$  for the scales of interest here with  $k\tau \gg 1$ . It is demonstrated below in this section that the perturbed ionization fraction  $\delta_{x_e}$  is of the same order of magnitude as  $\delta_b$  for the scales of interest. We therefore include perturbations to both the ionization fraction and the baryon density as the terms giving rise to second-order effects in the evolution equations.

It is easier to determine such second-order terms in real space. The relevant first-order equations to be modified are the  $\theta_b$  and  $\theta_\gamma$  formulae in equation (2), which in real space take the form

$$\begin{aligned} \dot{v}_b &= -\frac{\dot{a}}{a}v_b - c_s^2\nabla\delta_b - \nabla\psi + \frac{4\bar{\rho}_\gamma}{3\bar{\rho}_b}a\bar{n}_e\sigma_T(v_\gamma - v_b), \\ \dot{v}_\gamma &= -\nabla\left(\frac{1}{4}\delta_\gamma - \sigma_\gamma\right) - \nabla\psi + a\bar{n}_e\sigma_T(v_b - v_\gamma). \end{aligned} \quad (10)$$

Allowing for spatial fluctuations in the ionization fraction  $x_e$ ,

$$x_e = \bar{x}_e(1 + \delta_{x_e}), \quad (11)$$

the perturbations in the electron density then contain two terms arising from inhomogeneities in the baryon density and the ionization fraction, respectively:

$$n_e = \bar{n}_e(1 + \delta_{n_e}) = \bar{n}_e(1 + \delta_b + \delta_{x_e}). \quad (12)$$

We obtain the second-order contributions to the Thomson scattering terms in equation (10) by replacing  $\bar{n}_e$  with  $n_e$ ,  $\bar{\rho}_b$  with  $\rho_b = \bar{\rho}_b(1 + \delta_b)$ , and  $\bar{\rho}_\gamma$  with  $\rho_\gamma = \bar{\rho}_\gamma(1 + \delta_\gamma)$ :

$$\begin{aligned} \dot{v}_b &= -\frac{\dot{a}}{a}v_b - c_s^2\nabla\delta_b - \nabla\psi \\ &\quad + \frac{4\bar{\rho}_\gamma}{3\bar{\rho}_b}a\bar{n}_e\sigma_T(1 + \delta_{x_e} + \delta_\gamma)(v_\gamma - v_b), \\ \dot{v}_\gamma &= -\nabla\left(\frac{1}{4}\delta_\gamma - \sigma_\gamma\right) - \nabla\psi \\ &\quad + a\bar{n}_e\sigma_T(1 + \delta_{x_e} + \delta_b)(v_b - v_\gamma). \end{aligned} \quad (13)$$

We drop the second-order term containing  $\delta_\gamma$  in the  $\dot{v}_b$  equation because on small scales,  $\delta_\gamma \ll \delta_{x_e} \sim \delta_b$  due to photon diffusion damping. Transforming back to  $k$ -space, the nonlinear terms of  $O(\delta v)$  become convolutions, and we have

$$\begin{aligned} \dot{\theta}_b &= -\frac{\dot{a}}{a}\theta_b + c_s^2k^2\delta_b + k^2\psi + \frac{4\bar{\rho}_\gamma}{3\bar{\rho}_b}a\bar{n}_e\sigma_T(\theta_\gamma - \theta_b) \\ &\quad + \frac{4\bar{\rho}_\gamma}{3\bar{\rho}_b}a\bar{n}_e\sigma_Tk \int d^3k' [v_\gamma(k') - v_b(k')] \delta_{x_e}(|\mathbf{k} - \mathbf{k}'|), \\ \dot{\theta}_\gamma &= k^2\left(\frac{1}{4}\delta_\gamma - \sigma_\gamma\right) + k^2\psi + a\bar{n}_e\sigma_T(\theta_b - \theta_\gamma) \\ &\quad + a\bar{n}_e\sigma_Tk \int d^3k' \{[v_b(k') - v_\gamma(k')] \\ &\quad \times [\delta_{x_e}(|\mathbf{k} - \mathbf{k}'|) + \delta_b(|\mathbf{k} - \mathbf{k}'|)]\}, \end{aligned} \quad (14)$$

We also need an evolution equation for the ionization frac-

tion fluctuation  $\delta_{x_e}$ . It can be obtained by perturbing the zero-order ionization rate equation (5) (Liu et al. 2001),

$$\begin{aligned} \frac{d\delta_{x_e}}{d\tau} &= -aC_r \left[ \beta\delta_{x_e} + \bar{n}_H\alpha^{(2)}\bar{x}_e(\delta_b + 2\delta_{x_e}) \right] \\ &\quad + \left( \frac{\delta C_r}{C_r} - \delta_{x_e} \right) \frac{1}{\bar{x}_e} \frac{d\bar{x}_e}{d\tau}, \end{aligned} \quad (15)$$

where

$$\begin{aligned} \frac{\delta C_r}{C_r} &= -\Lambda_\alpha n_{1s} \beta^{(2)} \bar{n}_H [(1 - \bar{x}_e)\delta_b - \bar{x}_e\delta_{x_e}] \\ &\quad \times [\Lambda_\alpha n_{1s} + \Lambda_{2s \rightarrow 1s} \bar{n}_H (1 - \bar{x}_e)]^{-1} \\ &\quad \times \left\{ \Lambda_\alpha n_{1s} + [\Lambda_{2s \rightarrow 1s} + \beta^{(2)}] \bar{n}_H (1 - \bar{x}_e) \right\}^{-1}. \end{aligned} \quad (16)$$

We have assumed that  $\delta_{T_b} = 0$ , i.e., there are no perturbations induced in the baryon temperature. We verify this claim by including the perturbed evolution equation for  $T_b$  (Ma & Bertschinger 1995) in our calculations:

$$\begin{aligned} \frac{d(\delta_{T_b})}{d\tau} &= \delta_{T_b} \left( \frac{\dot{\bar{T}}_b}{\bar{T}_b} - \frac{2\dot{a}}{a} \right) \\ &\quad + \frac{8\bar{\rho}_\gamma\mu}{3\bar{T}_b m_e \rho_b} a\bar{n}_e\sigma_T [\delta_{x_e}(T_\gamma - \bar{T}_b) - \bar{T}_b\delta_{T_b}]. \end{aligned} \quad (17)$$

Here  $\mu$  is the mean molecular weight (including free electrons and all ions of hydrogen and helium) and  $T_b = \bar{T}_b(1 + \delta_{T_b})$ . We find that the value for  $\delta_{T_b}$  is always at least 2 orders of magnitude smaller than  $\delta_{x_e}$  because the source term  $(T_\gamma - T_b)$  for  $\delta_{T_b}$  is negligible until well into the recombination era. Even after recombination, the growth is not rapid enough to affect the evolution of  $\delta_{x_e}$ .

We note that the perturbation to the ionization fraction  $\delta_{x_e}$  arises naturally from the first-order cosmological equations and is not an ad hoc term. This perturbation is ignored in standard linear calculations because its effects on the photon and baryon evolution enter only at second order, as shown by equations (13) and (14). We show in the next section that numerical results from the linear theory indeed give comparable amplitudes for  $\delta_{x_e}$  and  $\delta_b$ . We are thus justified in keeping both the  $\delta_b v$  and  $\delta_{x_e} v$  terms in our second-order analysis.

### 3. NUMERICAL RESULTS

In this section we present results from numerical integration of the linear and second-order equations in § 2. The calculations are performed with the full Boltzmann code for the conformal Newtonian gauge in the COSMICS package (Ma & Bertschinger 1995; Bertschinger 1995). For the second-order results, modifications are made to this code to include the nonlinear terms in equation (14) and the perturbed rate equation (15). The matter density parameter is taken to be  $\Omega_m = 0.35$ , with  $\Omega_C = 0.30$  in CDM and  $\Omega_b = 0.05$  in baryons. The cosmological constant and Hubble parameter are  $\Omega_\Lambda = 0.65$  and  $h = 0.75$ . Three species of massless neutrinos and a helium fraction  $y = 0.24$  are assumed. The initial conditions are adiabatic Gaussian fluctuations with a spectral index of  $n = 1$ . All results are normalized to *COBE*.

### 3.1. Linear Evolution

Figure 1 illustrates the time evolution of the linear baryon density field  $\delta_b$  and CDM density field  $\delta_c$  for wavenumbers  $k = 1000, 2500, 5000,$  and  $10^4 \text{ Mpc}^{-1}$ . The corresponding masses are  $\sim 1000, 64, 8,$  and  $1 M_\odot$ , respectively. These scales are much smaller than the typically studied scales of  $k \lesssim 10 \text{ Mpc}^{-1}$  or  $M \gtrsim 10^9 M_\odot$ . We note two interesting features that are absent in the more familiar behavior of  $\delta_b$  at lower  $k$ . First, even though photon diffusion damping wipes out  $\delta_b$  very rapidly at  $z \sim 10^6\text{--}10^5$ ,  $\delta_b$  at such high  $k$  is able to grow before recombination because of the breakdown of photon-electron tight coupling on small scales. This rapid regenerative growth is characterized by a  $(1+z)^{-7/2}$  dependence and can be understood in terms of the balance achieved between the radiation drag force and the gravitational force (Yamamoto et al. 1998). As a result,  $\delta_b$  grows by at least 5 orders of magnitude before recombination ends at  $z \sim 1000$ . We also note a short period during recombination when  $\delta_b$  grows even more rapidly. This is because gravity is rapidly becoming the dominant force over the decreasing radiation drag force.

The second feature special to these high- $k$  modes is that they undergo a second Jeans-length crossing after recombination. It is well known that the baryonic Jeans wavenumber  $k_J = \lambda_J^{-1} \sim c_s^{-1}(4\pi a^2 G\rho)^{1/2}$  increases rapidly during recombination, reaching  $k_{J,\text{rec}} = 900(\Omega_m h^2)^{1/2} \text{ Mpc}^{-1} \approx 370 \text{ Mpc}^{-1}$  shortly after recombination for our model (Yamamoto et al. 1998). Perturbations with  $k > k_{J,\text{rec}}$ , which were Jeans unstable before recombination, become stable after recombination and exhibit oscillations due to the baryon thermal pressure. The growth of  $\delta_b$  is therefore

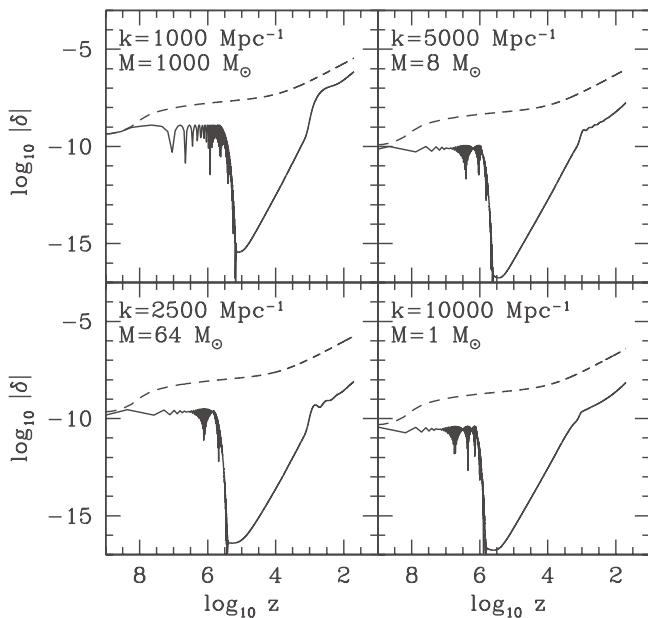


FIG. 1.—Time evolution of the linear baryon (*bottom curve*) and CDM (*top curve*) density field on very small scales:  $k = 1000, 2500, 5000,$  and  $10,000 \text{ Mpc}^{-1}$ . The results are computed in the conformal Newtonian gauge using the COSMICS Boltzmann code. The cosmological parameters are  $\Omega_C = 0.30, \Omega_b = 0.05, \Omega_\Lambda = 0.65,$  and  $h = 0.75,$  and the fluctuation amplitudes are normalized to *COBE*. Photon diffusion damping results in the sharp drop in the baryon amplitude at  $z \sim 10^6\text{--}10^5$ . This is followed by a power-law growth when the photon-baryon tight coupling becomes ineffective. The small oscillations after recombination at  $z \sim 1000$  in the high- $k$  modes are a result of the second Jeans-length crossing (see text).

slowed down as can be seen in Figure 1. As we show below, it is during this era when the small-scale perturbations are relatively constant that the second-order nonlinear term becomes important. When the Jeans wavenumber grows to the scale of a given  $k$ -mode, eventually the growth of  $\delta_b$  picks up again.

Figure 2 shows the linear power spectrum for the velocity difference ( $v_b - v_\gamma$ ) between the baryons and photons shortly after recombination. The Thomson scattering term is proportional to this quantity, which serves as the source term for the second-order effect to be discussed in the next section.

### 3.2. Nonlinear Evolution

We now solve the Einstein and Boltzmann equations, taking into account the second-order terms in equation (14). Two new features must be handled: the evolution of the perturbed ionization fraction  $\delta_{x_e}$  given by equation (15) and the  $k$  convolution in equation (14).

To compute  $\delta_{x_e}$ , we add equation (15) directly in the COSMICS Boltzmann code. We note that even though  $\delta_{x_e}$  is a first-order quantity and is of comparable amplitude to  $\delta_b$ , equation (15) was not included in the original linear COSMICS code because  $\delta_{x_e}$  contributes to the photon and baryon evolution equations only at second order. Figure 3 illustrates our numerical result for the time evolution of  $\delta_{x_e}$  for the  $k = 5000 \text{ Mpc}^{-1}$  mode. The dashed curve is for  $\delta_{x_e}$  computed from the linear theory. It indeed has a similar amplitude to  $\delta_b$  in Figure 1. Including the second-order terms in the calculations enhances the amplitude of  $\delta_{x_e}$  (*solid curve*), which peaks at a redshift of  $\sim 1000$ .

To handle the convolution terms in equation (14), we use the property that the velocity difference ( $v_\gamma - v_b$ ) in the integrand has significant contributions only from  $k' = 0.01$  to  $1 \text{ Mpc}^{-1}$ , as shown in Figure 2. This is much smaller than the  $k \gtrsim 1000 \text{ Mpc}^{-1}$  investigated in this paper. This allows us to

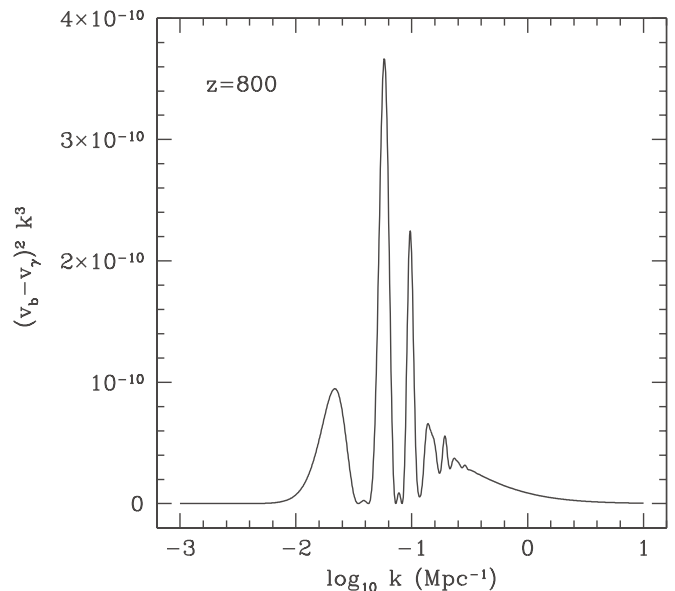


FIG. 2.—Linear power spectrum for the velocity difference between baryons and photons at redshift  $z = 800$ . The dominant contributions come from the modes in the range of  $k \sim 0.01\text{--}1 \text{ Mpc}^{-1}$ , which is much below the modes of interest in Fig. 1. This feature allows us to simplify the second-order velocity convolution terms in eq. (14).

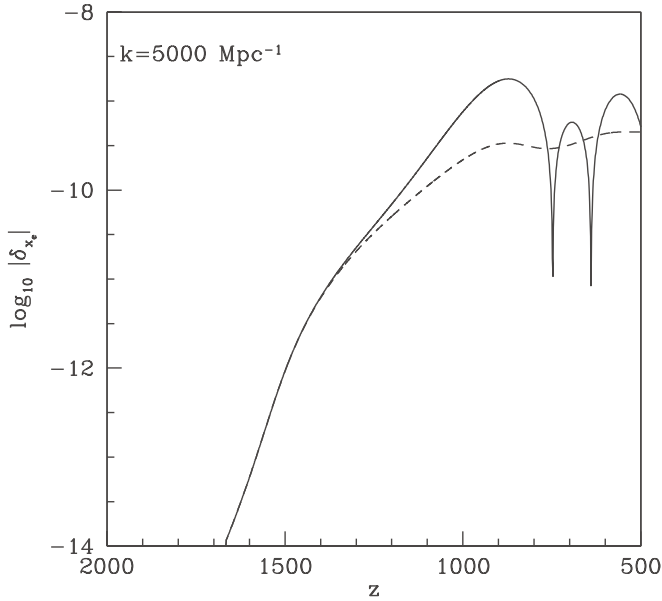


FIG. 3.—Perturbation to the ionization fraction  $\delta_{x_e}$  as a function of redshift, computed without (*dashed curve*) and with (*solid curve*) the second-order terms in eq. (14) for the velocity field  $\theta$ . The peak occurs at  $z \sim 1000$ , which is the same for all  $k$ -modes investigated.

take out  $\delta_{x_e}$  and  $\delta_b$  from the convolutions and approximate the velocity integral as

$$\int d^3k' [v_\gamma(k') - v_b(k')] \delta_{x_e}(|\mathbf{k} - \mathbf{k}'|) \approx \sigma_v \delta_{x_e}(k), \quad (18)$$

where

$$\sigma_v^2 = 4\pi \int d \ln(k') k'^3 [v_\gamma(k') - v_b(k')]^2. \quad (19)$$

Figure 4 shows  $\sigma_v$  as a function of redshift. Initially,  $\sigma_v$  is small because the tight coupling between baryons and photons keeps  $v_\gamma \approx v_b$ . As recombination proceeds and the tight coupling breaks down, the baryons fall into the CDM potential well, giving rise to the rapidly growing  $\sigma_v$  during  $z \sim 1500$ – $1000$ . For comparison, the long-dashed curve shows the baryon velocity alone. The agreement between the two curves shows that the photon velocity field  $v_\gamma$  is negligible after recombination. We approximate the time dependence of  $\sigma_v$  with the fitting formula

$$\log_{10} \sigma_v = -3.57 + 9.56 \times 10^{-4} z - 3.3 \times 10^{-6} z^2 + 1.126 \times 10^{-9} z^3, \quad (20)$$

shown as the short-dashed curve in Figure 4. This formula is used in the numerical integration for computational efficiency.

The results of our nonlinear calculations are illustrated in Figures 5–7. Figure 5 shows the time evolution of the linear versus nonlinear baryon density field  $\delta_b$  for a single mode  $k = 5000 \text{ Mpc}^{-1}$  of  $M \approx 10 M_\odot$ . The nonlinear  $\delta_b$  is calculated from the full Boltzmann code with the second-order convolution terms. The conformal time  $\tau$  is used for the horizontal axis to illustrate the postrecombination Jeans oscillations that are specific to these high- $k$  modes (see also discussions in § 3.1). It can be seen that  $\delta_b$  begins to oscillate immediately after recombination at  $\tau \approx 200 \text{ Mpc}$  because of the sharp decrease in the Jeans length. The time period

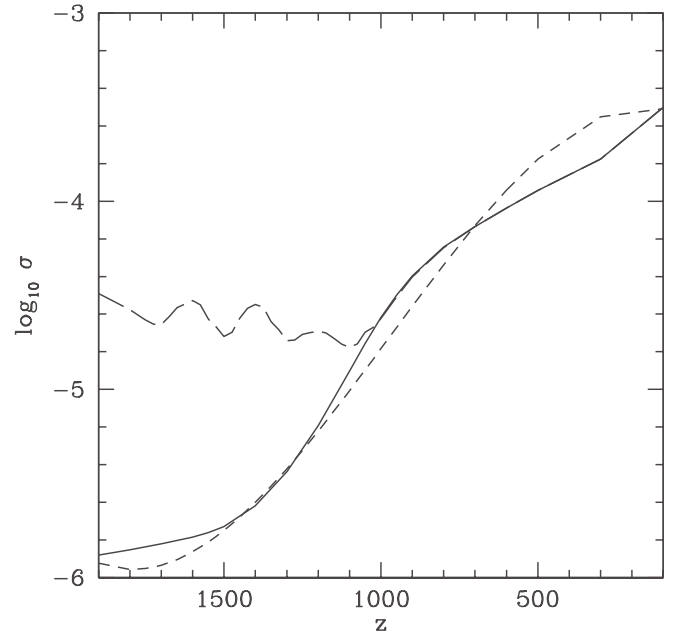


FIG. 4.—Evolution of  $\sigma_v$ , the rms of the baryon velocity  $v_b$  (*long-dashed curve*) and the rms of the baryon and photon velocity difference ( $v_b - v_\gamma$ ) (*solid curve*). The velocity difference is small at  $z \gtrsim 1500$  due to the tight coupling, but it increases rapidly during and after recombination when baryons and photons are no longer tightly coupled. The baryons subsequently fall into the potential well of the CDM, resulting in an increase in  $v_b$  and ( $v_b - v_\gamma$ ), whereas the photon perturbations simply diffuse away. The short-dashed curve shows the fitting formula for ( $v_b - v_\gamma$ ) used in our calculations.

of these oscillations is roughly  $2\pi/kc_s$ , where the baryon sound speed is related to the baryon temperature by  $c_s^2 = k_B T_b (1 - d \ln T_b / d \ln a / 3)$ . For  $k = 5000 \text{ Mpc}^{-1}$ , the baryons have  $T_b \sim 2500 \text{ K}$  at time  $\tau \sim 200 \text{ Mpc}$ , giving  $c_s \sim 1.5 \times 10^{-5}$  and  $\Delta\tau \sim 100 \text{ Mpc}$ , which agrees well with

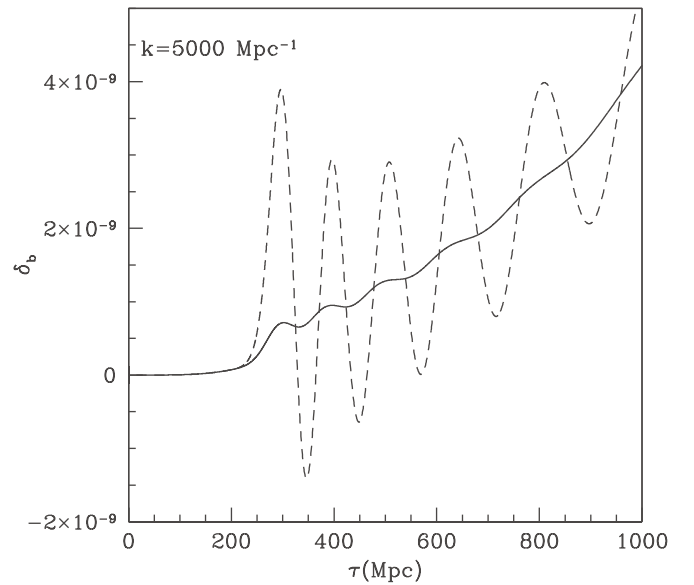


FIG. 5.—Linear (*solid curve*) vs. nonlinear (*dashed curve*) baryon density field  $\delta_b$  as a function of the conformal time  $\tau$  for the  $k = 5000 \text{ Mpc}^{-1}$  mode. The Jeans oscillations discussed in the text are clearly seen. The effect of the second-order terms is to increase the oscillation amplitude as well as to slightly shift the position of the peaks. The oscillation period is  $\sim 90 \text{ Mpc}$  immediately after recombination. The conformal time is  $\tau \approx 200 \text{ Mpc}$  at recombination and  $\tau_0 \approx 10^4 \text{ Mpc}$  today.

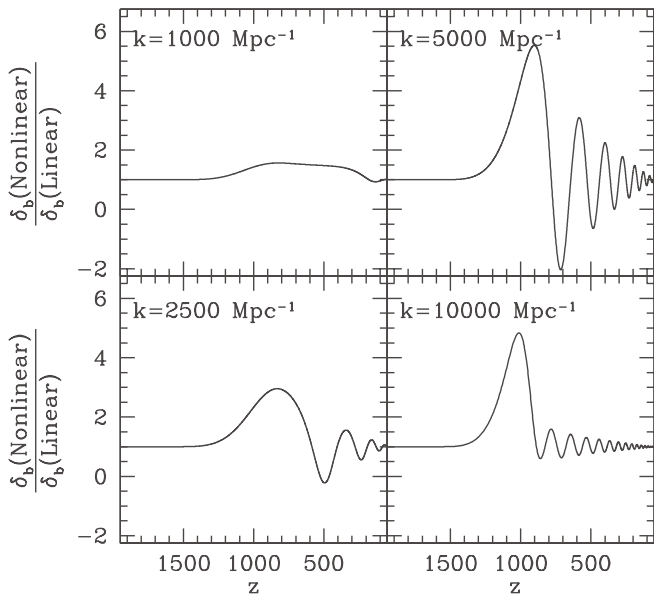


FIG. 6.—Ratio of the nonlinear and linear baryon density field  $\delta_b$  for four  $k$ -modes: 1000, 2500, 5000, and 10,000  $\text{Mpc}^{-1}$ . The oscillations in the ratio are more rapid for higher  $k$  modes due to the faster Jeans oscillations. The maximum amplitude reached by a particular  $k$ -mode is not a monotonic function of  $k$  but peaks between  $k = 5000$  and 10,000  $\text{Mpc}^{-1}$ . The oscillations die out and the effect of the nonlinear term decreases at low redshifts when other terms begin to dominate.

the periods of oscillations shown in Figure 5. Figure 6 shows the ratio of nonlinear and linear  $\delta_b$  for four wavenumbers:  $k = 1000, 2500, 5000,$  and  $10,000 \text{ Mpc}^{-1}$ . Figure 7 shows the same thing for the photon density field  $\delta_\gamma$ , which has a similar behavior as the baryons.

We find that the inclusion of the second-order terms has two main effects on the baryons: an increase in the amplitude of the Jeans oscillations and a slight shift in the sound speed, and hence the oscillation period. Both effects are clearly seen in the figures. The nonlinear enhancement reaches a maximum of a factor of several right after recom-

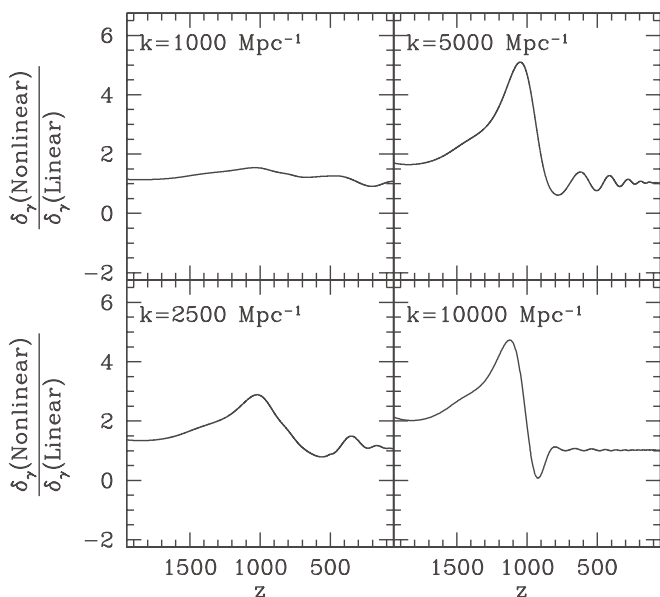


FIG. 7.—Same as Fig. 6, but for the photon density field  $\delta_\gamma$ . The behavior is qualitatively similar to the baryons in Fig. 6.

bination. It then decreases as the mean ionization fluctuation  $x_e$  decreases. The slight shift in the oscillation period is caused by the inclusion of perturbations to the ionization fraction. We have effectively introduced another term in the evolution equation for  $\theta_b$ , which together with the linear terms determines the period of the oscillations. The nonlinear coupling thus changes the time period of these oscillations to  $\sim 2\pi/(kc_s + \text{nonlinear effects})$ . This slight shift in the effective sound speed is the reason for the oscillations in Figures 6 and 7. It is also worthwhile to note that the maximum amplitude achieved by the ratio of the baryonic perturbations in the nonlinear theory compared with the linear calculation does not follow a simple relationship as a function of  $k$ . The amplitude of the ratio, for example, is larger for  $k = 5000 \text{ Mpc}^{-1}$  than for  $k = 10,000 \text{ Mpc}^{-1}$ . This is because the effect of the nonlinear term becomes less important as the frequency of the Jeans oscillations increases. For the particular cosmological model under consideration, this occurs at a scale between  $k = 5000$  and 10,000  $\text{Mpc}^{-1}$ .

#### 4. DISCUSSION

Figures 6 and 7 show that the second-order terms arising from the coupling of the large-scale baryon velocity fields to the perturbation in the electron ionization fraction on small scales dominate the evolution equation for the baryon-density perturbations  $\delta_b$  at  $z \sim 1000$ . This second-order effect dies off at lower  $z$ , however, and it does not push the small-scale baryon fluctuations into the nonlinear regime at a significantly earlier time, as was suggested by Shaviv (1998).

It is nevertheless interesting that for modes with  $k > 1000 \text{ Mpc}^{-1}$ , a second-order term can significantly alter the growth predicted by the linear theory right after recombination. How does any second-order term at  $z \sim 1000$  lead to an amplification of a factor of  $\sim 5$  in the linear baryon fluctuations, as we have found? To understand this, we plot in Figure 8 the time evolution of all the terms on the right-hand side of the  $\theta_b$  formula from equation (14):  $-\dot{\theta}_b/a$  (short-dashed curve),  $c_s^2 k^2 \delta_b$  (dotted curve),  $(4\rho_\gamma/3\rho_b)a\bar{n}_e\sigma_T(\theta_\gamma - \theta_b)$  (long-dashed curve), and the second-order term  $\sim v_b \delta_{x_e}$  (dot-dashed curve). Since the potential term  $k^2\psi$  is nearly a constant of time, it is convenient to normalize other terms to  $k^2\psi$ . To contrast the scale dependence of the nonlinear effect, we show two modes:  $k = 250$  and  $5000 \text{ Mpc}^{-1}$ . As one can see, the nonlinear effect is important only for the higher  $k$  mode. The nonlinear term is unimportant for the  $k = 250 \text{ Mpc}^{-1}$  mode because the pressure term  $k^2 c_s^2 \delta_b$  is small on these scales and cannot prevent the perturbations from growing under the influence of gravity. For the  $k = 5000 \text{ Mpc}^{-1}$  mode, however, the pressure term  $k^2 c_s^2 \delta_b$  keeps the perturbations in the terminal-velocity stage for a longer period of time (see Yamamoto et al. 1998). This leads to a near cancellation of all linear terms governing the growth of  $\theta_b$ . As a result, the second-order term gains importance and through the nonlinear coupling becomes the dominant term shortly after recombination. The effect of the coupling on the perturbed ionization fraction is shown in Figure 3, where the nonlinear coupling can give rise to an order-of-magnitude change in the value of  $\delta_{x_e}$ . At late times, the second-order term becomes negligible as the free-electron density  $\bar{n}_e$  becomes very small. We note that the Hubble drag term  $-\dot{\theta}_b/a$  is unimportant throughout because the scales of the perturbations under consideration are so small that they are not influenced by the large-scale expansion of the universe.

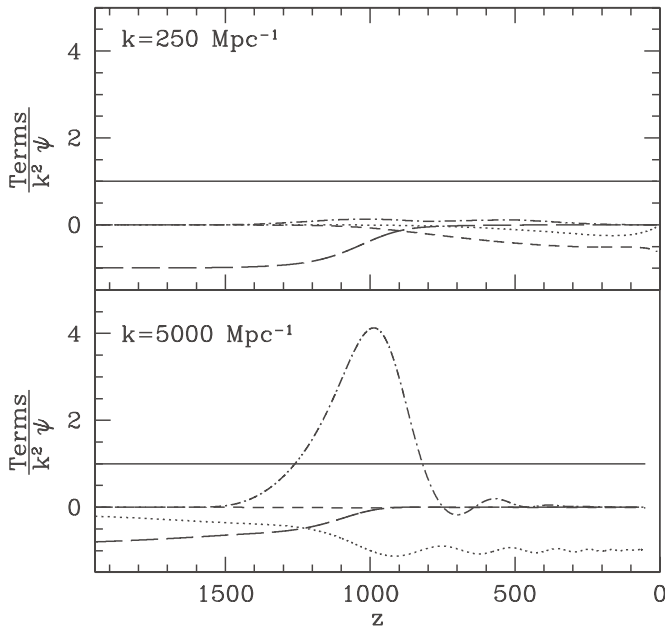


FIG. 8.—Amplitude of the individual terms on the right-hand side of the baryon velocity eq. (14) relative to  $k^2\psi$ :  $-\dot{\theta}_b/a$  (short-dashed curve),  $c_s^2 k^2 \delta_b$  (dotted curve),  $(4\bar{p}_\gamma/3\bar{p}_b)a\bar{n}_e\sigma_T(\theta_\gamma - \theta_b)$  (long-dashed curve), and the second-order term (dot-dashed curve). For the lower  $k$  mode, the second-order term is never important compared to the first-order terms. For  $k = 5000 \text{ Mpc}^{-1}$ , however, the near cancellation among the first-order terms at  $z \sim 1000$  allows the second-order term to dominate, leading to the nonlinear enhancement shown in Figs. 6 and 7. This figure illustrates how the second-order term becomes important for high- $k$  modes.

Our approach and results differ from the previous work on this subject (Liu et al. 2001) in a number of ways. We have solved the full set of Einstein and Boltzmann equations for the metric perturbations and the perturbation field in CDM, baryons, photons, and neutrinos. This approach has allowed us to calculate accurately the phase-space distribu-

tions of both baryons and photons. For the baryons, we find that the maximum amplitude reached by the nonlinear to linear ratio,  $\delta_b(\text{nonlinear})/\delta_b(\text{linear})$ , is similar to that of Liu et al. (2001) for  $k \lesssim 5000 \text{ Mpc}^{-1}$ , but our results show an oscillating ratio because the addition of the nonlinear coupling causes a change in the effective speed of sound. This effect was unnoticed in the work of Liu et al. (2001). In addition, their analysis finds a monotonic increase in the amplitude of the ratio as a function of  $k$ . We find instead that the maximum amplitude reached by the ratio for  $k = 10,000 \text{ Mpc}^{-1}$  is less than that for  $k = 5000 \text{ Mpc}^{-1}$ . This is again because their analysis was unable to track the Jeans oscillations after recombination accurately.

Our calculation has also included the nonlinear coupling terms in the evolution of the photon-density perturbations. As equations (13) and (14) show, two comparable nonlinear terms contribute to the photon velocity field:  $\delta_{x_e}(v_b - v_\gamma)$  and  $\delta_b(v_b - v_\gamma)$ . We have shown that the  $\delta_{x_e}(v_b - v_\gamma)$  term results in an initial enhancement of the amplitude for the baryons. Momentum conservation in Thomson scattering implies that this nonlinear term would tend to suppress the amplitude obtained from the linear calculation for the photons. It turns out that the  $\delta_b(v_b - v_\gamma)$  term is generally larger, and it acts in an opposite sense from the  $\delta_{x_e}(v_b - v_\gamma)$  term. The end result is an enhancement in  $\delta_\gamma$  as well, as shown in Figure 7. It may be an interesting future study to directly compute the angular power spectrum for the temperature fluctuations in the cosmic microwave background, but we expect the angular scales associated with the  $k \gtrsim 1000 \text{ Mpc}^{-1}$  modes to be at multipoles of  $l \gtrsim 10^6$ , below the scales probed by the current generation of experiments.

We thank Ue-Li Pen, Naoshi Sugiyama, and Thanu Padmanabhan for useful discussions. C.-P. M. acknowledges support of an Alfred P. Sloan Foundation Fellowship, a Cottrell Scholars Award from the Research Corporation, a Penn Research Foundation Award, and NSF grant AST 99-73461.

#### REFERENCES

- Bertschinger, E. 1995, COSMICS code release (astro-ph/9506070)  
Dodelson, S., & Jubas, J. M. 1995, ApJ, 439, 503  
Hu, W., Scott, D., & Silk, J. 1994, Phys. Rev. D, 49, 648  
Lifshitz, E. M. 1946, J. Phys. USSR, 10, 116  
Liu, G.-C., Yamamoto, K., Sugiyama, N., & Nishioka, H. 2001, ApJ, 547, 1  
Ma, C.-P., & Bertschinger, E. 1995, ApJ, 455, 7  
Mukhanov, V. F., Feldman, H. A., & Brandenberger, R. 1992, Phys. Rep., 215, 206  
Peacock, J. A. 1999, Cosmological Physics (New York: Cambridge Univ. Press)  
Peebles, P. J. E. 1968, ApJ, 153, 1  
———. 1980, The Large-Scale Structure of the Universe (Princeton: Princeton Univ. Press)  
Shaviv, N. J. 1998, MNRAS, 297, 1245  
Silk, J. 1968, ApJ, 151, 459  
Spitzer, L. 1978, Physical Processes in the Interstellar Medium (New York: Wiley)  
Weinberg, S. 1972, Gravitation and Cosmology (New York: Wiley)  
Yamamoto, K., Sugiyama, N., & Sato, H. 1998, ApJ, 501, 442